Dielectric Characteristics of Liquid Nitrogen/ Synthetic Paper Composite Insulation System for Extra High Voltage HTS Cable

N. Hayakawa, *Member, IEEE,* K. Yamakami, T. Masuda, and H. Kojima, *Member, IEEE*

***Abstract*—For extra-high-voltage high-temperature superconducting (HTS) cables, not only high electrical insulation performance but also low dielectric loss is required. Therefore, we focus on a porous synthetic paper with lower dielectric loss, e.g. Tyvek® polyethylene nonwoven fabric, than that of polypropylene laminated paper (PPLP®), which has been used for a conventional HTS cable insulation system. In this paper, we compare partial discharge inception characteristics for different liquid nitrogen/synthetic paper composite insulation systems. The partial discharge inception electric field strength in the composite insulation system depends on the electric field strength in the porous area of synthetic paper.**

***Index Terms*—Electrical insulation, HTS cable, liquid nitrogen, synthetic paper, volume effect**

I. Introduction

HIGH temperature superconducting power cables are expected to transmit large amount of electricity with lower transmission losses than conventional power cables. In Japanese M-PACC project, a 275 kV high-temperature superconducting (HTS) cable has been developed with the highest voltage level in the world. The dielectric loss of 0.6 W/m of the 275 kV HTS cable was three times larger than the AC loss of 0.2 W/m in superconducting conductor [1]. For the insulation system of such an extra-high-voltage HTS cable, not only high electrical insulation performance but also low dielectric loss performance is required. Therefore, we have focused on a porous synthetic paper with lower dielectric loss, e.g. Tyvek® polyethylene (PE) nonwoven fabric produced by DuPont™, than that of polypropylene laminated paper (PPLP®) produced by TOMOEGAWA, which has been used for a conventional HTS cable insulation system [2], [3]. The dielectric loss factor $\varepsilon_r \tan\delta$ of Tyvek® is 20% of that of PPLP®. However, the electrical insulation characteristics of liquid nitrogen (LN_2)/synthetic paper composite insulation system with the mechanism of partial discharge inception have not been sufficiently understood yet.

In this paper, we investigate the dielectric characteristics of Tyvek®, the Tyvek® laminated with PE film on one side (Tyvek®/PE), the PE film laminated with Tyvek® on both sides (Tyvek®/PE/Tyvek®), and PPLP® in LN_2. We discuss the partial discharge inception characteristics of the LN_2/synthetic paper composite insulation system for the partial discharge inception mechanism in terms of volume effect.

(Corresponding author: Naoki Hayakawa.)
N. Hayakawa, K. Yamakami, T. Masuda, and H. Kojima are with Nagoya University, Nagoya, 464-8603, Japan (e-mail: nhayakaw@nagoya-u.ac.jp, yamakami@hayakawa.nuee.nagoya-u.ac.jp, masuda@hayakawa.nuee.nagoya-u.ac.jp, kojima@nuee.nagoya-u.ac.jp).

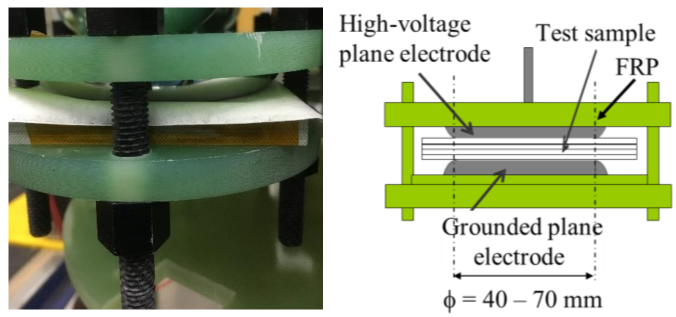

(a) Parallel plane electrodes

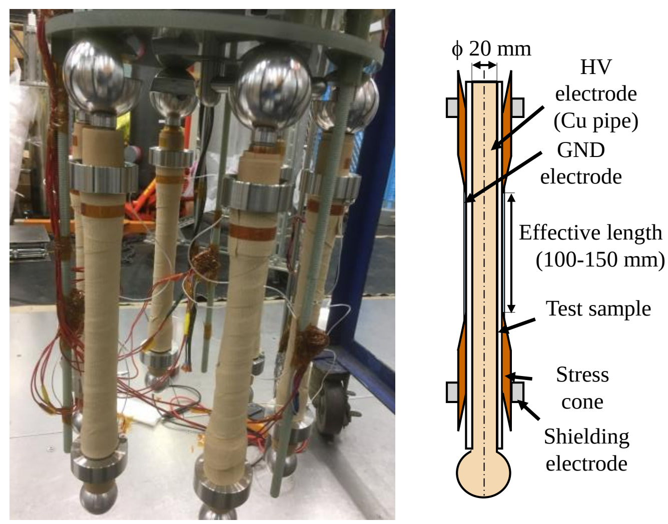

(b) Cable model

Fig. 1. Configuration of sample electrode system.

II. Experimental

A. Electrode System

As the electrode system for evaluating dielectric characteristics of the composite insulation system, we used a parallel

TABLE I
SPECIFICATIONS OF INSULATION PAPER

	Tyvek®	Tyvek®/PE	Tyvek®/PE/Tyvek®	PPLP®
Thickness t (mm)	0.091–0.148	0.128–0.154	0.227–0.247	0.116–0.125
Basis weight M (g/mm^2)	(0.64–0.76)×10^{-4}	(0.85–1.06)×10^{-4}	(1.75–1.77)×10^{-4}	(1.04–1.10)×10^{-4}
Void ratio β (%)	22.1–53.6	27.2–40.0 (without PE film)	23.7–31.2 (without PE film)	34.6–41.0 (without PP film)
		17.0–35.6 (with PE film)	18.0–24.8 (with PE film)	20.8–24.6 (with PP film)
Stack number	4–8	2–8	1–8	2–8
LN_2 volume V_{LN2} (mm^3)	121–2376	205–1382	62–3910	88–2141

TABLE II
TRUE DENSITY AND RELATIVE PERMITTIVITY IN LN_2 OF EACH MATERIAL

	Tyvek®	Kraft paper	Polyethylene (PE)	Polypropylene (PP)
ρ (g/mm^3)	0.95	1.5	0.95	0.90
ε_r	1.8	2.5	2.3	2.2

plane electrode system and a cable model as shown in Fig. 1. In the parallel plane electrode system, one to eight insulation papers were sandwiched between the plate electrodes with the diameter of 40 or 70 mm. In the cable model, insulation paper was wrapped up around the center conductor with the diameter of 20 mm, and the effective length was 100–150 mm. Specifications of the insulation paper are shown in Table I. Basis weight M (g/mm^2) was calculated from measured insulation paper area S (mm^2) and mass m (g) of insulation paper by (1). Void ratio β (%), LN_2 volume inside the insulation paper V_{LN2} (mm^3), and possible and equivalent volume of microscopic bubbles V_{Bubble} (a.u.) in insulation paper were determined as follows:

$$M = m / S \tag{1}$$
$$\beta = 1 - M / (\rho \cdot t) \tag{2}$$
$$V_{LN2} = \beta V + V_B \tag{3}$$
$$V_{Bubble} = V_{LN2} \cdot 0.1 / P \tag{4}$$

where ρ (g/mm^3) and t (mm) are the true density and the thickness, respectively, V (mm^3) is the volume of insulation paper, V_B (mm^3) is the volume of butt gap that is considered in the cable model, and P (MPa) is the pressure of LN_2. V_{Bubble} has been normalized by V_{LN2} at 0.1 MPa.

B. *Setup and Measurement Method*

Fig. 2 shows the experimental setup. The cryostat consists of double vessel; the inner vessel can be pressurized and the outer vessel is kept in atmospheric pressure. Six samples can be set in the cryostat, and we can select the tested sample to which a high voltage is applied in LN_2. The inner and outer vessels were filled with LN_2, and the LN_2 in the inner vessel was pressurized by filling nitrogen gas. Therefore, the pressure of LN_2 in the inner vessel was controlled in the range of 0.1–0.3 MPa under constant temperature of 77 K.

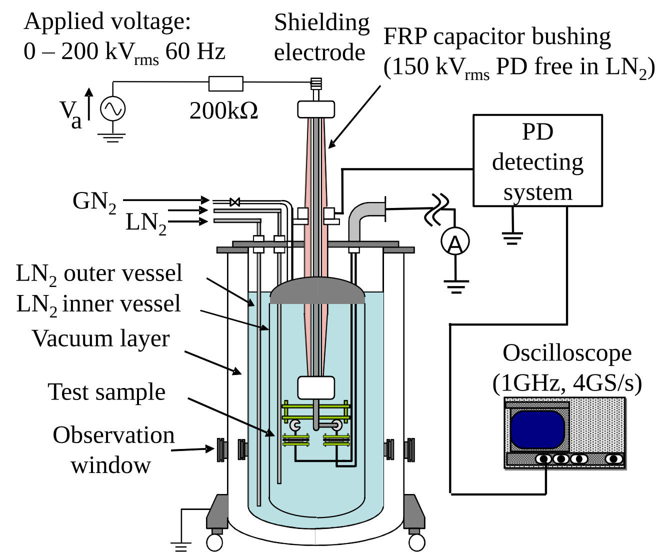

Fig. 2. Experimental setup.

A high AC voltage of 60 Hz was applied to the electrode system in the cryostat with the increasing rate of 1 kV_{rms}/s, and the partial discharge inception voltage (PDIV) was obtained ten times. The partial discharge inception electric field strength (PDIE) was evaluated from the PDIV by the several methods as discussed in the following section. The partial discharges were detected by a CR circuit system composed of capacitors and resistors with the detection sensitivity of 5 pC.

III. RESULTS AND DISCUSSION

A. *Evaluation Method of Partial Discharge Inception Electric Field Strength in LN_2/synthetic Paper Composite Insulation System*

Firstly, in Fig. 3a, we evaluate PDIE of the sample at the partial discharge inception by the average electric field strength $PDIE_{LN2}$ in LN_2, which is calculated by a simplification of the porous sample with a parallel plate capacitor based on the volume ratio of LN_2 in the insulation paper, as shown in Fig. 4a [4]. Fig. 3a shows the dependence of PDIE on V_{Bubble} for each insulation paper. In Fig. 3, the dotted line indicates the 95% confidence interval, the dashed line indicates the 95% prediction interval, and the error bar of each plot denotes the

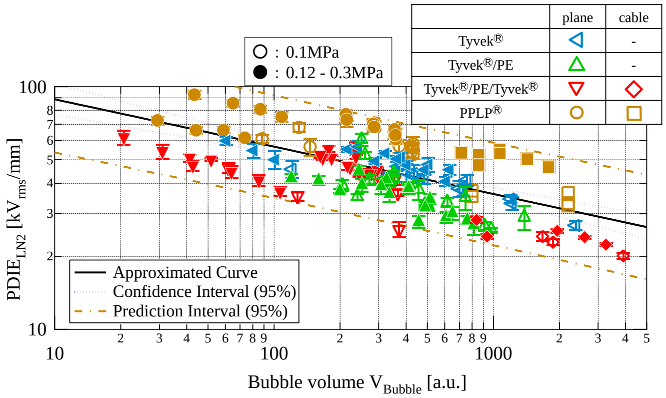

(a) PDIE$_{LN2}$

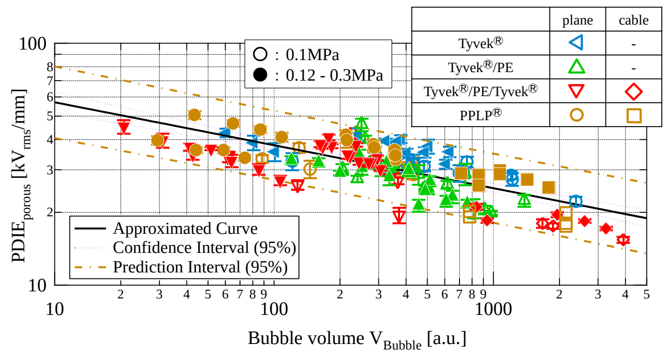

(b) PDIE$_{porous}$

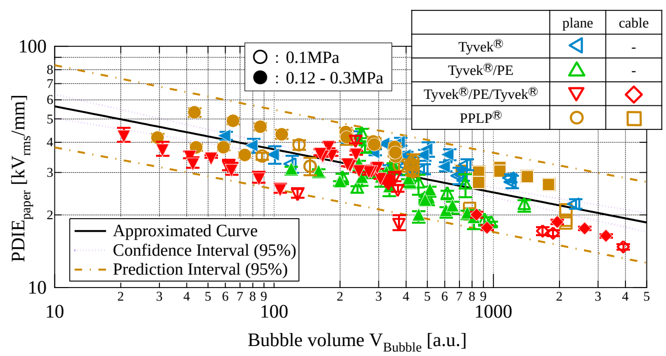

(c) PDIE$_{paper}$

Fig. 3. PDIE strength of LN_2/synthetic paper composite insulation system as a function of V_{Bubble}.

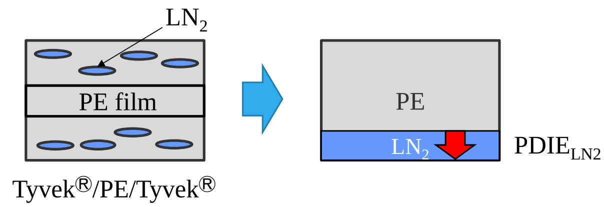

(a) PDIE$_{LN2}$

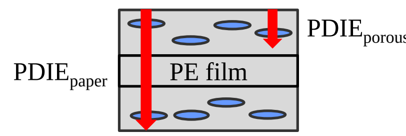

(b) PDIE$_{porous}$, PDIE$_{paper}$

Fig. 4. Evaluation models of PDIE.

standard deviation. PDIE$_{LN2}$ of each sample linearly decreases with the increase of V_{Bubble} in a log-log graph. This implies the volume effect, which is a decrease of PDIE with the increase of the liquid nitrogen volume, i.e. an increase of weak points on the electrical insulation. On the other hand, PDIE$_{LN2}$ of PPLP® in Fig. 3a tends to be higher than PDIE$_{LN2}$ of synthetic paper. However, since PDIE$_{LN2}$ means the electric field strength applied to LN_2, it should not be affected by the material of insulation paper. Hence, we consider that PDIE$_{LN2}$ cannot correctly represent partial discharge inception characteristics in LN_2/synthetic paper composite insulation system.

Next, we evaluate PDIE by PDIE$_{porous}$ and PDIE$_{paper}$ shown in Fig. 4b. PDIE$_{porous}$ is the average electric field strength in the porous paper calculated by using the relative permittivity of each material in LN_2 as shown in Table II [5], [6]. On the other hand, PDIE$_{paper}$ is the average electric field strength in the whole sample obtained by simply dividing PDIV by the total thickness. Figs. 3b and 3c show the dependence of PDIE$_{porous}$ and PDIE$_{paper}$ on V_{Bubble}. In Figs. 3b and 3c, the PDIE$_{porous}$ and PDIE$_{paper}$ of PPLP® are almost the same as those of other samples. This will mean that PDIE$_{porous}$ and/or PDIE$_{paper}$ are more suitable than PDIE$_{LN2}$ for the evaluation of partial discharge inception characteristics. Furthermore, the correlation coefficients of PDIE$_{LN2}$, PDIE$_{porous}$, and PDIE$_{paper}$ with V_{Bubble} are 0.628, 0.747, and 0.693, respectively, that is PDIE$_{porous}$ has the highest correlation coefficient. In addition, the prediction interval of PDIE$_{porous}$ is the narrowest; therefore, PDIE$_{porous}$ can most accurately represent the partial discharge inception characteristics. This may be because LN_2 impregnated in a void of porous insulation paper makes the weak point in electrical insulation, while LN_2 is not impregnated into the high-density film, such as PE and PP.

The above results suggest that PDIE$_{porous}$ and V_{Bubble} are important indicators of the partial discharge inception characteristics in LN_2/synthetic paper composite insulation system.

B. Volume Effect of Partial Discharge Inception Electric Field Strength in LN_2/synthetic Paper Composite Insulation System

As discussed above, partial discharge in LN_2/synthetic paper composite insulation system is caused in LN_2 inside the sample. On the other hand, in a LN_2 gap under quasi-uniform electric field, it is considered that a dielectric breakdown occurs immediately after a partial discharge inception. Therefore, in this section, we compare the partial discharge inception characteristics in LN_2/synthetic paper composite insulation system with the breakdown characteristics in a LN_2 gap.

The dielectric breakdown of LN_2 depends on the electrically stressed liquid volume with potential weak points as the origin of breakdown, i.e. microbubbles in LN_2. Since the potential of microbubbles depends on the size and number of microbubbles as the origin of breakdown existing in the region with high electric field strength, the stressed liquid volume (SLV)

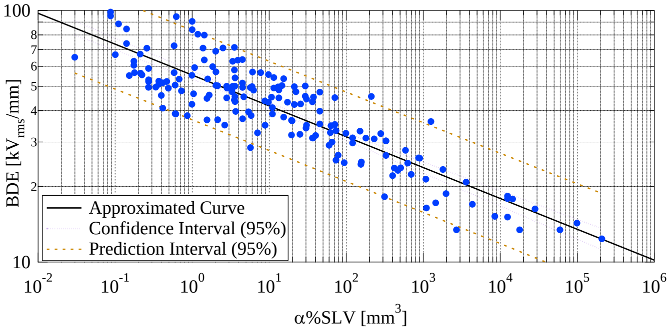

Fig. 5. Breakdown strength of LN_2 gap as a function of *α%SLV*.

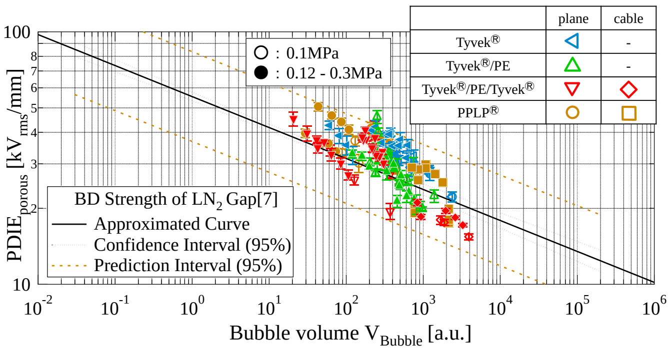

Fig. 6. Volume effect of PDIE for LN_2/synthetic paper composite insulation system.

with the potential of breakdown decreases with the pressure rise and/or temperature decrease of LN_2. In our previous work, the authors have formulated the breakdown electric field strength *BDE* (kV_{rms}/mm) in a LN_2 gap under quasi-uniform electric field by the following equation [7]:

$$BDE = 55.4\cdot(\alpha\%SLV)^{-1/8.15} \quad (5)$$

where *α%SLV* (mm^3) means the stressed liquid volume with the electric field strength higher than α (%) of the maximum electric field strength. The value of α is a function of the pressure and temperature of LN_2, e.g. α = 81% at atmospheric pressure and α = 89% at 77 K, 0.3 MPa. Fig. 5 shows the dependence of *BDE* on *α%SLV* in LN_2 at 65–77 K, 0.1–0.3 MPa [7]. *BDE* linearly decreases in a log-log graph with increasing of *α%SLV*. This means the volume effect of *BDE* in LN_2.

In the LN_2/synthetic paper composite insulation system described in the previous section, $PDIE_{porous}$ also depends on the stressed liquid volume inside the insulation paper including voids; this tendency is similar to the volume effect of *BDE* in LN_2 gap. For directly comparing the volume effect in the LN_2/synthetic paper composite insulation system with that of *BDE* in LN_2 gap, we assume that *α%SLV* (mm^3) = V_{Bubble} (a.u.). This assumption means that the discharge is initiated by microbubbles in LN_2 even in the synthetic paper. Fig. 6 shows the dependence of $PDIE_{porous}$ on V_{Bubble} shown in Fig. 3b with the approximated curve, the 95% confidence interval, and the 95% prediction interval of *BDE* in LN_2 gap in Fig. 5 based on the above assumption. As can be seen from Fig. 6, $PDIE_{porous}$ is in the range of the 95% prediction interval of *BDE* in LN_2 gap. This result agrees with the estimated mechanism in previous section; namely, partial discharge in LN_2/synthetic paper composite insulation system is caused by microbubbles as weak point in the porous area inside the insulation paper impregnated with LN_2.

IV. Conclusion

This paper has described the dielectric characteristics of the liquid nitrogen/synthetic paper composite insulation system for extra-high-voltage superconducting cables, and investigated the volume effect of the partial discharge inception electric field strength in synthetic paper in atmospheric pressure and pressurized liquid nitrogen. The main results in this paper as follows:

1) The partial discharge inception characteristics depends on the average electric field strength of the insulation paper part with voids and equivalent volume of microscopic bubbles V_{Bubble}. This suggests that liquid nitrogen inside insulation paper with voids is a weak point in electrical insulation, and its electric field strength and volume are important indicators.
2) The volume effect of the partial discharge inception electric field strength in the liquid nitrogen/synthetic paper composite insulation system is similar to that of the dielectric breakdown in liquid nitrogen gap. This implies that the partial discharge in the liquid nitrogen/synthetic paper composite insulation system is caused by microbubbles in porous area inside the insulation paper impregnated with liquid nitrogen.

These results enable us to design the extra-high-voltage superconducting cables with low dielectric loss and high dielectric strength by using the porous papers such as Tyvek®, while understanding their mechanisms in terms of volume effect.

References

[1] O. Maruyama, T. Ohkuma, T. Masuda, Y. Ashibe, S. Mukoyama, M. Yagi, T. Saitoh, T. Hasegawa, N. Amemiya, A. Ishiyama, and N. Hayakawa, "Development of 66 kV and 275 kV class REBCO HTS power cables," *IEEE Trans. Appl. Supercond.*, vol. 23, no. 3, Jun. 2013, Art. no. 5401405.

[2] N. Hayakawa, S. Nishimachi, O. Maruyama, T. Ohkuma, J. Liu, and M. Yagi, "A novel electrical insulating material for 275 kV high-voltage HTS cable with low dielectric loss," *J. Phys.: Conf. Ser.*, vol. 507, May 2014, Art. no. 032021.

[3] R. Zuijderduin, "Integration of high-Tc superconducting cables in the Dutch power grid of the future," Ph.D. dissertation, Dept. Elect. Sustainable Energy, TU Delft, Delft, The Netherlands, 2016.

[4] N. Hayakawa, K. Ishida. T. Matsuoka, and H. Kojima, "Electrical insulation characteristics and mechanisms of low dielectric loss materials for high-voltage HTS cables," *IEEE Trans. Appl. Supercond.*, vol. 27, no. 4, Jun. 2017, Art. no. 4800904.

[5] S. Mukoyama, M. Yagi, T. Yonemura, and T. Nomura, "Superconducting cable," Japanese Patent 5877153, Mar. 2, 2016.

[6] H. Ichikawa, N. Fujiwara, M. Yagi, and S. Mukoyama, "Properties of insulation materials for a high voltage HTS power cable," in *2010 Annu. Meeting Rec. I.E.E. Japan*, Tokyo, 2010, p. 126.

[7] N. Hayakawa, S. Nishimachi, H. Kojima, and H. Okubo, "Size effect on breakdown strength in sub-cooled liquid nitrogen for superconducting power apparatus," *IEEE Trans. Dielectr. Electr. Insul.*, vol. 22, no. 5, pp. 2565–2571, Oct. 2015.